DOI: https://doi.org/10.68732/e138a48b5028b20c

ISBN: 978-9989-2053-6-1

Application of Auxetic reinforced mortar elements for pressurized tunnels

Arsham Moayedi Far
Institute of Subsurface Engineering, Montanuniversität Leoben, Leoben, Austria
arsham.moayedi-far@unileoben.ac.at
0000-0001-9802-9693

Marlene Villeneuve
Chair of Subsurface Engineering, Montanuniversität Leoben, Leoben, Austria

Giuseppe Loporcaro
Department of Civil and Environmental Engineering, University of Canterbury, Christchurch, New Zealand

Abstract

Designing pressurized underground tunnels requires mobilizing confinement from the surrounding rock mass by establishing an effective lining–rock bond; conventionally this is achieved via pressure grouting the annular gap to prestress a stiff steel or concrete lining, but an alternative is a flexible lining that deliberately accommodates larger displacements and develops this bond as internal pressure rises. We investigate this flexible concept using auxetic-reinforced mortar samples, composites that couple mortar infill with 3D-printed auxetic lattices fabricated from nylon filament reinforced with 15% carbon fiber. Auxeticity is the property of materials that have a negative Poisson's ratio, meaning they expand laterally when stretched and contract laterally when compressed. Because direct tensile testing of these composites is challenging, we characterized mechanical performance using splitting tests. Compared with conventional materials, auxetic-reinforced specimens exhibited substantially higher ductility under splitting conditions. Results also show that auxetic geometry and mortar–polymer interfacial strength govern stiffness, post-cracking behaviour, and failure modes. Moreover, the auxetic systems exceed the highest circumferential strain threshold of conventional linings by orders of magnitudes. These findings support a shift from stiff, brittle linings to ductile, auxetic-enabled flexible linings that can deform and expand circumferentially to engage rock confinement in pressurized storage tunnels.

Keywords

Underground pressurized tunnels; Auxetic structures, Flexible linings.

1 Introduction

Under high internal water pressure, tensile stresses can exceed the lining's tensile strength, causing cracking and potential leakage (Dadashi et al. 2017). For high heads in competent rock, prestressed concrete linings are adopted, typically using pressure grouting to induce compressive hoop prestress that counteracts fluid-induced hoop tension (Wang et al. 2020). Steel linings are an alternative for high pressures, yet they are costly, challenging to construct, and susceptible to buckling under high external groundwater pressures, especially during emptying; this necessitates added thickness beyond that required for internal pressure alone (Wang et al. 2020).

These challenges motivate the development of lining materials that combine tensile strength with enhanced ductility (Moayedi Far and Villeneuve 2025) to better mobilize confinement from the surrounding rock mass. Such solutions could complement prestressing, reduce or eliminate grouting, and enhance lining performance. Given demonstrated gains in ductility, toughness, and tension capacity, auxetic concepts are a promising direction.

Auxetic materials exhibit a negative Poisson's ratio, expanding laterally when stretched (Evans et al. 1991). This behaviour underpins superior functional properties versus conventional materials, including improved indentation resistance, higher shear stiffness, enhanced fracture toughness, and greater energy absorption (Carneiro et al. 2013; Evans and Alderson 2000; Alderson et al. 1994). Owing to their rarity in nature, research has focused on auxetic-based composites, typically an auxetic reinforcing framework with a matrix filler, for structural applications requiring combined deformability and strength (Carneiro et al. 2013), including, base isolation, and concrete reinforcement (Zhang and Yang 2016; Gu et al. 2022).

Cementitious materials are economical and strong in compression but brittle in tension, with low energy absorption and limited resistance to impact and vibration; reinforcement strategies using steel, synthetic fibers, and recently auxetic concepts have been explored to overcome these limits (Mukhopadhyay and Khatana 2014; Momoh et al. 2021).Recent studies further substantiate these trends. Xu et al. (2024) developed an auxetic cementitious composite (ACC) by combining 3D-printed Thermoplastic Polyurethane auxetic structures with mortar, achieving strain hardening, recoverable cyclic deformability, and improved energy dissipation over conventional and fiber-reinforced concretes. Chen et al. (2024) examined engineered cementitious composites where the auxetic structure itself is cementitious; their "buckling-induced" auxetic lattices showed higher compressive strength, energy absorption, flexural strength, and toughness than comparable re-entrant and cross-chiral forms. These findings point to auxetic composites as viable solutions for applications requiring toughness, energy absorption, and controlled deformation.

This research aims to investigate the performance of two types of auxetic reinforced mortar samples when subjected to indirect uniaxial tensile testing, providing insights into the applicability of such structures for pressurized tunnels. As specimen geometry, size effects, and equipment differences can strongly influence the results of direct uniaxial tension (Ouyang et al., 2024), the splitting test, an indirect method, has been employed in this investigation. To position these structures relative to conventional options, a comparison based on the induced circumferential strain is also presented. Together, these analyses assess the potential of auxetic reinforced mortar structures for use in pressurized tunnel environments.

2 Lining Design for pressurized tunnels

In pipeline design, the minimum wall thickness is determined by internal pressure, pipe radius, allowable material stress, temperature, and a joint-related coefficient (Antaki 2003). The allowable stress is set at 72% of the material's specified minimum yield strength at the design temperature and is independent of the material's ultimate strength (Antaki 2003). Because yield strength differs among materials (e.g., steel, unreinforced concrete, reinforced concrete), the allowable radial and circumferential strains, and thus the permissible expansion, are material dependent. In pressurized tunnels and underground spaces, this allowable deformation dictates how much the lining can expand to engage the surrounding rock, and any remaining gap is typically filled with pre-stress grouting to ensure contact between the rock mass and the tunnel lining, since conventional linings have limited allowable strain (Fernández 1994).

For pressure tunnels, sections are classified by potential leakage into: (1) sections where hydrojacking or hydrofracturing of the rock mass can occur, and (2) sections where the in-situ stress in the rock mass is high enough to prevent these phenomena (Fernández 1994).

For zones of high hydrojacking and/or hydrofracturing potential, a steel liner must be installed at all locations where the minimum in-situ stress is below 1.3 times the internal tunnel pressure under normal operation (Benson 1986; Brekke and Ripley 1986). In flat areas with marginal in-situ stresses where some leakage can be tolerated, and slope instabilities are unlikely, a heavily reinforced concrete liner can be considered as an alternative to long steel liners.

In areas where in-situ stresses are sufficient, whether a liner is needed primarily depends on the rock mass permeability, the acceptable level of leakage, and the ground pore-water pressures that can be safely induced without triggering instability in the surrounding materials (Fernández 1994). If a liner is required to limit leakage or to reduce excess pore-water pressures outside the tunnel, its effectiveness is governed by the ratio of its permeability with respect to the permeability of the surrounding media (Fernández 1994). Since the permeability of concrete liners is strongly influenced by the circumferential strain developed after pressurization, the magnitude of that strain should be used as a key index for selecting the appropriate liner type (Fernández 1994).

When the rock mass is relatively permeable (rock mass hydraulic conductivity in excess of 1×10^{-5} cm/s), the preferred liner type can be selected based on the circumferential strain induced by the internal tunnel pressure. The following design guidelines are from Fernández (1994):

1. Plain concrete when circumferential strain is less than 1.5×10^{-4}, combined with thorough contact grouting to achieve a relatively "impermeable" barrier.
2. Plain concrete plus consolidation grouting for strain up to 4×10^{-4}; grout hole lengths should be about the tunnel radius or slightly longer, and injection pressures should be at least equal to the internal tunnel pressure.
3. Reinforced concrete for a strain more than 4×10^{-4}.
4. Reinforced concrete with a plastic membrane for strain more than 6×10^{-4}.
5. Concrete liner incorporating a thin steel membrane for strain exceeding 8×10^{-4}.

If the tunnel's internal pressure is high and/or the surrounding ground has relatively low stiffness, the thin steel membrane in option 5 may need to be thickened to avoid buckling under external loads (Fernández 1994). Once the required thickness reaches this point, it is more appropriate to design a conventional steel liner (Fernández 1994).

When the rock mass has low permeability (less than 1×10^{-5} cm/s), installing plain or reinforced concrete liners, whether or not accompanied by consolidation grouting, does little to reduce tunnel leakage or limit induced pore-water pressures in the surrounding ground (Fernández 1994). However, rock with these properties is typically tight and massive, so leakage rates are inherently low. If the rock is nonerodible and not prone to dissolution or deterioration, and the formation is massive and sound, the excavation may be left unlined. The following suggestions are from Fernández (1994):

1. Concrete with nominal reinforcement when the surrounding rock is vulnerable to erosion or deterioration and the liner's circumferential strain is above 6×10^{-4}.
2. Reinforced concrete when the rock is susceptible to dissolution and the circumferential strain exceeds a value of 3×10^{-4}.

If the design requires a stricter control of leakage or pore-water pressures, an embedded impermeable barrier within the concrete liner can be used. Depending on the anticipated circumferential strain in the liner, this barrier may be a plastic membrane or a thin steel sheet (Fernández 1994).

To illustrate this, we consider a tunnel with internal pressure of 10 (MPa), inner radius of 2.5 (m), concrete lining thickness of 0.5 (m), Elastic modulus of 30 (GPa), Poisson ratio of 0.2, and shrinkage strain coefficient of 0.0005 (m/m). Concrete shrinkage causes a radial displacement of -1.5×10^{-3} (m) and hoop strain of -5×10^{-4}. Based on Lame's solution the expansion due to internal pressure would lead to radial displacement of 4.36×10^{-3} (m) and hoop strain of 1.52×10^{-3}. Summing the opposing strains and displacements, the lining would be subjected to expansion with radial displacement of 2.86×10^{-3} (m) and strain of 1.02×10^{-3}.

For the lining to successfully close the gap, the allowable radial expansion would need to be higher than the radial shrinkage of concrete and the lining material would need to be able to handle the induced hoop strain. Even the concrete liner incorporating a thin steel membrane with hoop strain capacity of 8×10^{-4} is unable to provide enough capacity, warranting the exploration of auxetic composites for this function.

3 Materials and methods

3.1 Printing Auxetic Structures

Two auxetic lattice designs, a re-entrant pattern and a missing-rib pattern, were developed and printed for this study. Unit cells were configured to cubic specimens of 40×40×40 mm for splitting tests. All lattices were fabricated using a Prusa i3 MK3S+ with a nylon filament reinforced with 15% carbon fibers, selected for its high strength, toughness, stiffness and resistance to impact, heat, and abrasion.

3.2 Sample preparation

To accommodate the complex auxetic geometries and small specimen sizes, a fine mortar was prepared using quartz sand with particle size<0.5 mm. The mix comprised ordinary Portland cement 865 (kg/m^3), quartz sand (<0.5 mm, 865 kg/m^3), Silica fume (192 kg/m^3), water(218 kg/m^3) and a superplasticizer (38 kg/m^3). Dry constituents (cement, sand, microsilica) were blended for 3–5 minutes. After blending the dry ingredients, approximately 70–80% of the total water was slowly incorporated. The remaining water, pre-mixed with the superplasticizer, was then added, and mixing continued for about five minutes until the mixture became uniform and highly workable. The fresh mortar was cast into molds containing the auxetic lattices, consolidated on a lab vibrator for 1–2 minutes, and stored under humid room conditions. After 24 hours, re-entrant and missing-rib reinforced mortar specimens (MrARC, ReARC) (Fig. 1) were demolded and water cured for 28 days (Moayedi Far et al., 2026).



Fig. 1 Cubic samples; a) MrARC, b) ReARC. (Moayedi Far et al., 2026).

3.3 Laboratory tests

Splitting tests were performed on an MTS 815 servo-hydraulic machine under displacement control to obtain full load–displacement responses. The auxetic-reinforced specimens were tested ata constant rate of 0.35 mm/min. A 2D digital image correlation (DIC) setup was used to obtain full-field surface displacements by correlating reference images with video frames captured during testing. The camera was placed 25 cm from the speckled specimens and aligned parallel to the specimen's surface normal to reduce out-of-plane error.

4 Results and insights

4.1 Splitting tests

Fig. 2 shows force–horizontal strain responses for all specimens in which the strain values were obtained from DIC. The auxetic-reinforced specimens highlight a significant ductility, with both ReARC and MrARC reaching a maximum horizontal strain of about 29%. In terms of peak load, MrARC records the lowest (5.673 kN), whereas ReARC attains the highest mean force (11.577 kN).

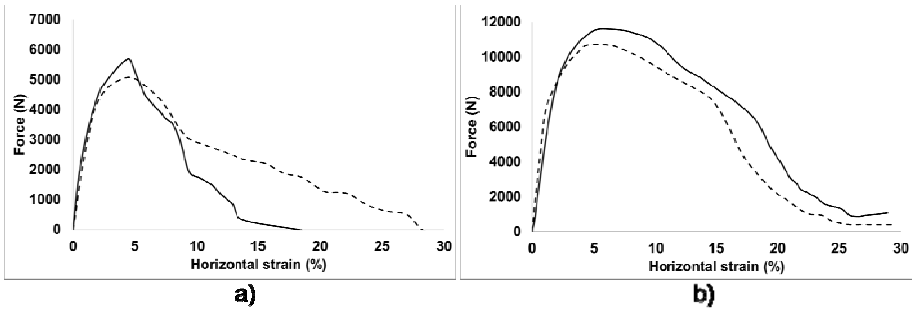


Fig. 2 Force-horizontal strain for a) MrARC and b) ReARC.

Post-failure, for MrARC, the dominant weakness plane forms through coalescence of cracks within the mortar and dilation/offset at the mortar–auxetic interface, which steers the final split(Fig. 3a). In ReARC, auxetic cells near the rollers deform in tension and bending, concentrating damage in the adjacent mortar; the upper mortar is crushed, the lower region near the roller shows fracture growth, and dilation at the mortar–auxetic interface creates the final dominant failure plane (Fig. 3b).



Fig. 3 Final state of a) MrARC and b) ReARC.

4.2 Insights

In splitting tests, the ReARC response is dominated by the auxetic lattice, with the mortar contributing mainly in the regions adjacent to the rollers. A weak mortar–auxetic interface establishes the dominant weakness plane, while the lattice sustains a complex stress state combining tension and shear. ReARC attains higher splitting strength than MrARC, largely because the auxetic members near the rollers are preferentially activated, mobilizing the high tensile capacity of the ePAHT CF lattice; this localized effect elevates the overall load-bearing capacity.

Geometric and interfacial characteristics distinguish MrARC from ReARC. The MrARC pattern (with edges) promotes broader stress transfer and engages more mortar elements, so its capacity depends on the combined performance of mortar and lattice rather than on localized lattice action. In contrast, the simpler ReARC topology makes the global response more sensitive to interface quality; stronger bonding tends to concentrate load transfer through the lattice near the rollers, whereas weaker bonding promotes more independent deformation of the two phases and a larger affected region.

The auxetic-reinforced mortars reached high pre-first-peak tensile strains, MrARC$4.7\times10^{-2}$and ReARC5.3×10^{-2}. Thus, the auxetic systems exceed the concrete liner incorporating a thin steel membrane limit (circumferential strain of 8×10^{-4}) by nearly two orders of magnitude. This increased ductility could close larger gaps and accommodate the induced hoop strainwithout or with minimal additional measures (e.g., grouting).

5 Conclusion

Based on the experimental results, the following conclusions can be drawn:

1. Auxetic-reinforced specimens experience a mixed stress state during splitting tests.
2. Auxetic geometry controls how much of the sample is engaged in tests and how strongly mortar participates.
3. Mortar–lattice bond quality has a significant effect of the level of involvement of accrete cells and failure plane in the samples.
4. Auxetic-reinforced specimens show significant improved ductility.
5. The added ductility could help underground storage linings expand to close the rock–lining gap during pressurization compared to other conventional alternatives.

Acknowledgment

This work was supported by the New Zealand government (MBIE contract UOCX2207) under the Endeavour program "Pūhiko Nukutū: a green hydrogen geostorage battery in Taranaki" and by the Hydrogen Under Ground (HUG) project funded by Business Finland's Co-Research instrument and project partners. An instance of GPT-4 within Academic AI was used for language enhancement; the authors reviewed and edited the content and assume full responsibility. Auxetic samples were printed by Mr. Stephan Schuschnigg, Department of Polymer Engineering and Science, Montanuniversitaet Leoben.

References

Alderson KL, Pickles AP, Neale PJ, Evans KE (1994) Auxetic polyethylene: the effect of a negative Poisson's ratio on hardness. Acta Metallurgica et Materialia 42 (7): 2261–2266. https://doi.org/10.1016/0956-7151(94)90304-2

Antaki GA (2003) Piping and pipeline engineering: design, construction, maintenance, integrity, and repair. 1st edn. CRC Press, Boca Raton

Benson RP (1986) Design of steel lined penstocks and high pressure power tunnels. Proceedings of the 5th Canadian Tunnelling Conference, Niagara Falls, Canada, 1986

Brekke T, Ripley B (1986) Design strategies for pressure tunnels and shafts. Rep. EPRI contract No. RP-1747. Electric Power Research Institute, Palo Alto

Carneiro VH, Meireles J, Puga H (2013) Auxetic materials—A review. Materials Science-Poland 31 (4): 561–571.

Chen M, Fang S, Wang G, Xuan Y, Gao D, Zhang M (2024) Compressive and flexural behaviour of engineered cementitious composites based auxetic structures: An experimental and numerical study. Journal of Building Engineering 86: 108999. https://doi.org/10.1016/j.jobe.2024.108999

Dadashi E, Noorzad A, Shahriar K, Goshtasbi K (2017) Hydro-mechanical interaction analysis of reinforced concrete lining in pressure tunnels. Tunnelling and Underground Space Technology 69: 125–132.

Evans KE, Alderson A (2000) Auxetic materials: functional materials and structures from lateral thinking! Advanced Materials 12 (9): 617–628.

Evans KE, Nkansah MA, Hutchinson IJ, Rogers SC (1991) Molecular network design. Nature 353 (6340): 124–124. http://dx.doi.org/10.1038/353124a0

Fernández G (1994) Behavior of pressure tunnels and guidelines for liner design. Journal of Geotechnical Engineering 120 (10): 1768–1791.

Gu JB, Wang JY, Lu W (2022) An experimental assessment of ultra high performance concrete beam reinforced with negative Poisson's ratio (NPR) steel rebar. Construction and Building Materials 327: 127042.

Moayedi Far A, Villeneuve M (2025) Towards a Safe and Large-scale Solution for Balancing Renewable Energy Supply and Demand. BHM Berg-und Hüttenmännische Monatshefte 170 (12): 766-773.

Momoh EO, Osofero AI, Menshykov O (2021) Bond behaviour of oil palm broom fibres in concrete for eco-friendly construction. Proceedings of the Institution of Civil Engineers – Construction Materials 174 (1): 47–64. https://doi.org/10.1680/jcoma.19.00097

Mukhopadhyay S, Khatana S (2015) A review on the use of fibers in reinforced cementitious concrete. Journal of Industrial Textiles 45 (2): 239–264. https://doi.org/10.1177/1528083714529806

Ouyang X, Huang Y, Hu X, Yin J, Shi C (2024) Evaluation of tensile failure behavior of ultra high performance concrete under double-edge wedge splitting and direct tension loadings. Journal of Building Engineering 90: 109480.

Wang H, Shao J, Zhang W, Yan Z, Huang Z, Liang X (2023) Three-point bending response and energy absorption of novel sandwich beams with combined re-entrant double-arrow auxetic honeycomb cores. Composite Structures 326: 117606. https://doi.org/10.1016/j.compstruct.2023.117606

Wang X, Liu L, Fu R, Sun X (2020) Newly developed pressure adaptable concrete lining for high pressure hydraulic tunnels. Tunnelling and Underground Space Technology 105: 103570.

Xu Y, Meng Z, Bol RJ, Šavija B (2024) Spring-like behavior of cementitious composite enabled by auxetic hyperelastic frame. International Journal of Mechanical Sciences 275: 109364. https://doi.org/10.1016/j.ijmecsci.2024.109364

Zhang XW, Yang DQ (2016) Numerical and experimental studies of a light-weight auxetic cellular vibration isolation base. Shock and Vibration 2016 (1): 4017534. https://doi.org/10.1155/2016/4017534

Moayedi Far, A., Villeneuve, M., Loporcaro, G., & Schuschnigg, S. (2026). Compressive mechanical behavior and energy absorption of auxetic reinforced cementitious elements. Construction and Building Materials, 538, 147278. https://doi.org/10.1016/j.conbuildmat.2026.147278